Optics Communications 284 (2011) 2633–2637

Contents lists available at ScienceDirect

Optics Communications

journal homepage: www.elsevier.com/locate/optcom

Full field deformation measurement of centimeter sized objects using optical phase retrieval

B. Gombkötő *, R. Séfel, J. Kornis

Department of Physics, Budapest Universtiy of Technology and Economics, Budapest, Hungary

ARTICLE INFO

Article history:
Received 27 May 2010
Received in revised form 5 January 2011
Accepted 25 January 2011
Available online 15 February 2011

Keywords:
Phase retrieval
Interference
Wave propagation

ABSTRACT

Most papers in the field of optical phase retrieval either consider only the intensity (or amplitude) profile of the object under inspection (or scatterer location in the X-ray version), or a uniform tilt/rotation of the object beam. However, phase retrieval is able to recover the phase profile of the object (beam) as well, which theoretically makes the observable interference of phase retrieved object waves possible. In this paper we demonstrate this principle experimentally on centimeter sized deformable reflective objects (as large as 40 mm by 40 mm) and corresponding simulations are also presented. When the CCD camera is moved along the optical axis in the Fresnel region, the interference fringes of the displacement field have low contrast. On the other hand, when an imaging setup is built, and the camera moves near the image plane, high fringe contrast can be obtained. These fringes however suffer from some phase error. In our work the iterative modulus projection algorithm was used as a simply implementable phase retrieval method.

1. Introduction

With the appearance of high resolution digital cameras, spatial light modulators and powerful desktop computers digital holography became a well established experimental and measurement tool in optical non-destructive testing [1–3]. The holographic principle, which encodes the phase of a beam into intensity modulation, opens many ways of digital wave manipulation techniques to improve interferometric applications, such as direct phase difference calculation instead of phase stepped intensity fringe processing, comparative measurement of two real objects [4], comparison with an ideal simulated object [5], or tilt compensation in shape measurement. The cost of a holographic optical setup is however the vibration free environment needed within an interferometric precision range.

Another possibility of obtaining the phase of an optical beam using a digital camera is to record multiple intensity patterns of the same beam. These intensities can be Fourier pairs, Fresnel pairs, which require a lens in the optical setup, or a sequence of intensities within a limited range of motion along the main propagation direction of the beam. Processing these recordings in the computer one can estimate the corresponding phase of the beam numerically [6,7]. The physical picture behind these calculations is clear: the same intensity pattern with two different phase patterns results in different intensity patterns at a distant location due to wave propagation, while intensity and phase together, or better said the complex amplitude is what propagates.

Once the phase of the beam is known, it can be propagated using numerical diffraction formulas in the computer and focusing may occur, which will tell the location of point sources ("bright pixels"), e.g., the object amplitude or intensity profile can be reconstructed. Another application is tilt or direct angle measurement of plane or spherical beams, which is sometimes called as wavefront sensing [8], and the setup usually contains a small iris.

For the estimation of the beam phase several algorithms are known in the literature. In most cases an iterative approach is used due to their relatively simple implementation. When only two constraints (image plane and Fourier plane intensity measurements) are used, more sophisticated combinations of them are also known, such as the hybrid input–output (HIO) algorithm [9], or the relaxed averaged alternating reflections (RAAR) algorithm [10]. The constraints or projection can also vary: a relaxation parameter can be introduced, and noisy or saturated pixels can be omitted. A direct solution to phase retrieval is also known when two axially displaced intensity patterns and thus the corresponding first derivative is known [11].

The aim of this paper is to demonstrate another possible use of phase retrieval. Interferometric fringes of a centimeter sized diffuse object are produced from two sequences of intensity recordings made before and after the surface of the object is deformed/displaced due to an applied load. Simulation and experimental results are presented, and the optical setup and its parameters are discussed.

* Corresponding author at: H-1111 Budapest, Budafoki út 8., Hungary. Tel.: +36 14631457; fax: +36 14634180.
E-mail addresses: gombkoto@eik.bme.hu (B. Gombkötő), richard.sefel@gmail.com (R. Séfel), kornis@eik.bme.hu (J. Kornis).

0030-4018/$ – see front matter © 2011 Elsevier B.V. All rights reserved.
doi:10.1016/j.optcom.2011.01.072

2. Overview and details of the optical setup

Imagine the simple optical setups in Fig. 1. An expanded and collimated beam is illuminating the object having a matte white paint surface, and the scattered objective speckle field is recorded in multiple (10–20) positions of the camera along the optical axis. After the phase retrieval calculation the objective speckles will also have a corresponding phase, and by applying a discrete Fresnel transform the obtained complex amplitude can be back propagated into the object plane, and an image of the original object will be seen. Now thinking of continuous signals, if the phase of the optical wave is known somewhere far away from the sources (the object surface), it is also known in the object/image plane by some extent. Considering also the aperture effect of the finite sized CCD camera, the phase in this plane must have a general curvature due to this aperture, and a superimposed random phase which can be related to the object surface itself. Displaying this phase distribution as a wrapped grayscale image will not show any information useful for the human eye or an image processing algorithm. Having geometrical parameters typical in digital holography, when the object size is several centimeters, the sampling distance (pixel size) in the object plane will be several tens of micrometers due to the discrete Fresnel transformation, which means that the optical wave itself is not really resolved, i.e., the output of the Fresnel transform cannot be further propagated.

But the same conditions hold for digital holography as well, yet interferometry is possible there, if the diffraction orders of the digital hologram are separated in the reconstruction plane due to the non-in-line (but small angle) arrangement. If one records a set of intensity patterns in an initial state of the object and another set after a load is applied, and the object is deformed (surface elements are displaced), the two sets can be the input of a phase retrieval calculation, and the two output complex amplitudes in one of the camera planes will be the intermediate result. These two phase retrieved waves (complex wavefields) added or subtracted, i.e., their interference field can be propagated back to the object plane, and there an interferometric fringe system will appear. (Of course the addition or subtraction of the waves can be performed in the object plane as well, but since the Fresnel transform/free space propagation is linear, the previous method is advantageous.) Considering the subtraction of the two resulting waves, the general wavefront curvature due to the aperture effect of the CCD will be canceled, and only the object related phases and their difference will influence the final fringe system.

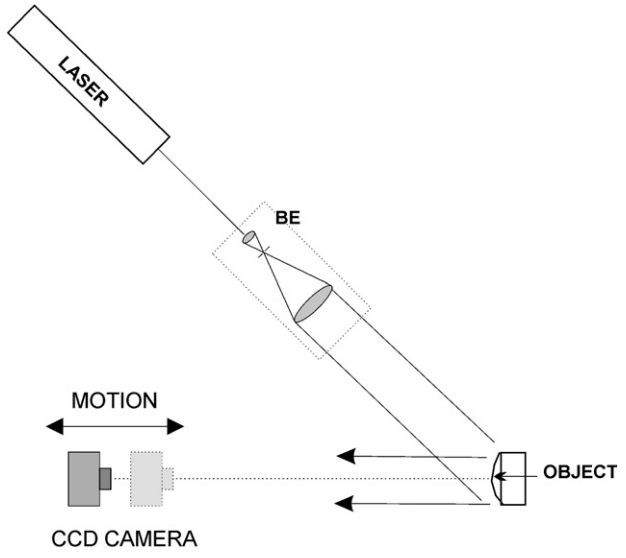

Fig. 1. Optical setup of the non-imaging (lensless) case of phase retrieval (BE = beam expander).

The interpretation of the fringes will be the same, as in holographic interferometry. The illumination and the observation directions define a sensitivity vector, and according to other known arrangements out-of-plane, in-plane displacement fields, or also shape could be measured [12]. The main question regarding fringe patterns generated this way is that how perfect phase retrieval is, when not only the amplitude of the object is important (location and strength of the point sources), but (relative) phase as well. The effectiveness of phase retrieval naturally depends not only on the applied method but also on the input intensity patterns. If the measurement aims several centimeter sized objects, and a naked CCD camera is used, many experimental limiting factors will restrict our possibilities.

Given a CCD pixel size of approximately 5 μm, the minimum object-to-camera distance should be much larger than the object size—typically more than 50 cm—to fulfill the sampling condition. The required mechanical tolerance of the motion stage in the direction perpendicular to the motion should be negligible, i.e., smaller than the pixel size. This limits the range of the motion itself pretty much: in our experiments this was within 5 cm. To avoid stagnation during the iterative phase retrieval in the setup in Fig. 1, more than two recordings are needed. The more the input patterns available, the better the results expected, but the runtime of the iteration is increasing, so recording more than 20 images is not practical. The stepping distance of the motion stage also has an ideal value. If it is too small, successive recordings show almost the same objective speckle pattern; thus, the change in the information content of the patterns is small. At least half the longitudinal size of the objective speckles is advised, or a distance close to the entire size. If the steps of motion are too large, we may not be able to record enough patterns within the available range of motion.

One important measure of the setup is the ratio of the motion range to the minimum object-to-camera distance. If this ratio is higher, much more is seen from the “propagation” of the beam, and phase retrieval will be more accurate. Considering this principle an ideal setup would be where the camera starts directly next to the object, or even if the camera would move around the object symmetrically, intersecting it in the middle of the motion range. Naturally, in these cases one of the recording planes would coincide with many or all of the point sources of the beam, so their location would be known exactly, but there will be even more information available, while a corresponding phase will be retrieved using all the other recordings. As a conclusion, having such a “near-field” arrangement a really good result may be expected, or thinking of the interferometric measurement we are aiming, the visibility or contrast of the final fringe system will be high.

In fact, such experimental setups are impossible to make, but it is possible to model it in a computer. Another experimental option is to image the object using a lens, as shown in Fig. 2, and to move the camera near the image plane. Recording defocused images and possibly one focused image is already known in the literature to reconstruct an object [13], but to our knowledge this method was not used to laser illuminated diffusely scattering objects. The obvious advantage of the imaging setup is that the image formed by the lens can be considered a secondary object, which is of course band limited according to the F# of the lens, but if the magnification of the imaging geometry is set properly, the object is will be sampled at many points. In this picture we may say that the camera scans the “near field” of this secondary object, and the location of the secondary point sources will be known precisely, and hopefully also their phases. Another advantage is that the original size of the object is no longer a matter, but the size of its image is what counts. As the speckle field behind the lens is subjective, to fulfill the sampling criterion the F# is typically set to 11 or 16. Both the lensless and the imaging setup has a limiting aperture, the CCD detector and the lens aperture correspondingly; thus, for a given amount of load on the object the correlation of the speckle fields passing the apertures and the highest value of the final fringe contrast will be limited. As the presented optical setups are similar to those of digital holography and speckle interferometry

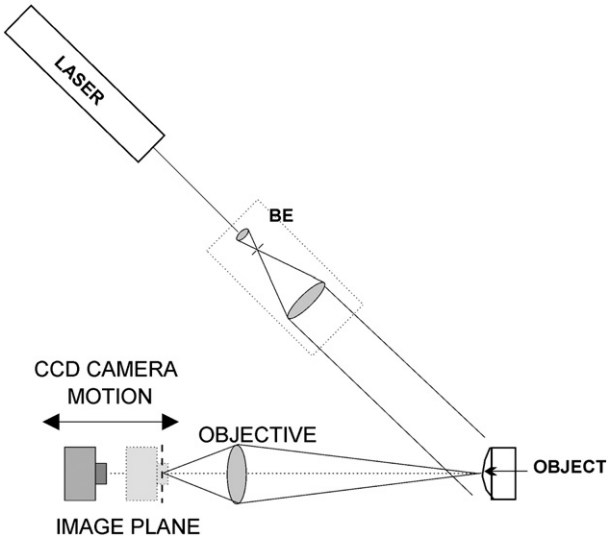

Fig. 2. Optical setup of the imaging case of phase retrieval (BE = beam expander).

(ESPI) but omitting a second reference arm, the fringe contrast/visibility we may expect can be high.

3. Applied phase retrieval method

If there are multiple intensity recordings available, not just two, and these were recorded "near" each other (neither Fourier nor Fresnel transformation should be used to propagate between the recording planes), using a so-called modulus projection is preferred [6,7,13]. Briefly described, the iteration starts with one of the recordings, an initial uniform phase is set, and then after every propagation step (calculated using the Fourier based convolution or with other terminology the angular or plane wave spectrum propagator method) the resulting intensity is replaced with the recorded one, and the phase of the wave is kept. As the determination of phase is based on intensity measurement, some additional conditions may be added, such as omitting overexposed (gray level 255) and low intensity (e.g., gray levels 0–4) noisy pixels from the replacement. Another known improvement is partly replacing and partly keeping the intensity in a linear combination, which is a different relaxation of the iteration. According to experiences a relaxation parameter of 0.7–0.8 is advised in contrast to 1, which would mean total replacement. Finally, intensities or grayscale values that turn out to be more than 255 and are not replaced by any measured intensity value (in an 8-bit case) are cut back to this maximum. (To avoid the actual corruption of intensity profiles, exposure parameters in the experiment should be chosen adequately in order to keep the ratio of these later omitted pixels only a few percent.) When using the plane wave spectrum propagator, edge effects may inflict proper diffraction modeling, therefore a satisfactory zero padding of the matrices is applied in the calculation. Putting together all of these known techniques the iteration is more effective, than the original basic modulus projection.

4. Simulation results

The parameters in the simulation were matched to some of our experimentally available devices. The CCD detector was a 1280×1024 pixel Baumer Optronics MX-13 camera with $6.7\,\mu m\times6.7\,\mu m$ pixel spacing. Only a 1024×1024 pixel sized area of the images was processed. A continuous wave He–Ne laser was used at 632.8 nm wavelength and cca. 50 mW power. The illumination was an expanded plane wave being non-normal to the object surface, as seen in Figs. 1 and 2. In the simulations the illumination was considered to be normal. In some cases an 8-bit quantization of floating-point data was introduced to imitate the 8-bit dynamic range of the real camera, but this had little effect. Fringe visibility in this paper is meant to be the standard ratio of modulation depth and mean value. For curved fringes this was estimated visually (reading approximated minimum and maximum value) from a linear intersection of the fringe pattern, while in the case of parallel fringes a sinusoidal function was fitted onto a cumulated fringe plot. (The single variable plot/function is generated by adding intensities along the uniform fringe directions.)

4.1. Far-field setup

Fig. 3 shows interferometric fringes in a simulation. Part a) of the figure shows the difference of the two retrieved waves in the object plane, and part b) of the figures shows the corresponding sum of the waves. The parameters of the setup are the following: the object size is $20\text{ mm}\times20\text{ mm}$, the number of recordings is 2×10, the step length is 5 mm, and the object-to-camera distance is 100–105 cm. The visibility of the fringes is approximately 0.2–0.3, which could be used very limited in fringe processing algorithms. The complementary fringes of the two parts in the figure prove that the intensity modulation seen is due to the interference of the two waves. Furthermore, in part a) of the figure the remaining zero order spot (while phase retrieval is imperfect) of the image is canceled out as expected, similar to digital holographic interferometry.

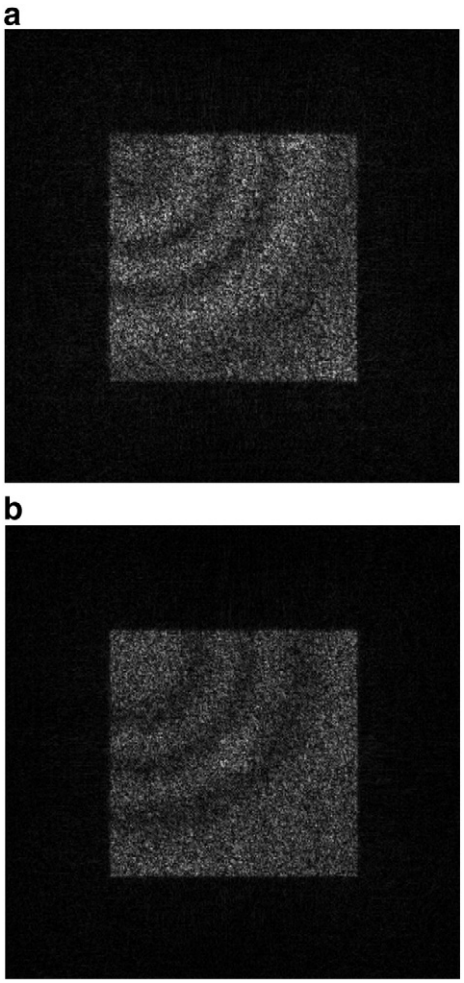

Fig. 3. Complementary (phase shifted) interference patterns of a deformed object in a far-field simulation. The fringe visibility is about 0.2–0.3.

4.2. Near-field setup

Fig. 4 shows (parallel) interferometric fringes of a rigid body rotation in a "near-field" simulation, where the object to camera distance was −10–10 mm. The object size was 1 mm×1 mm, and 2×20 recordings were used with a 1 mm step length. The visibility of the fringes is above 0.9 after 400 iteration steps per wave. While this is the setup, which is experimentally impossible (the camera cannot intersect the object, i.e., there is no place for illumination), this high visibility only predicts that in an experiment the imaging setup in Fig. 2 will enable us to have high fringe visibilities. Fig. 5 shows the convergence of the iteration by measuring the fringe visibility as the algorithm proceeds. In this case the object to camera distance was 0 to 40 mm and 2×40 recordings were used with a 1 mm step length, but the object was the same as above. The "500 steps" point of the curves corresponds to the visibility of the original fringes of the two complex waves, i.e., the "target" of phase retrieval, and represent the upper limit of the curves, to which they should converge. It is seen in Fig. 5 that convergence is not always monotonic, and it depends both on surface roughness (speckle intensity statistics) and tilt angle of the object. These curves support what is known from the literature as the case that the phase of partially developed speckle fields [14] can be retrieved more effectively (there are less phase vortices, where the intensity is zero) and therefore it is advantageous to inspect objects having smaller surface roughness or to use short coherence length lasers. Care must be taken, while in our aimed interferometric measurements speckles are the key information carriers about the object surface, so a completely incoherent speckle free illumination is not applicable. Using a LED illumination and recording far-field intensity patterns in a lenless setup is not enough to obtain a focusable wave.

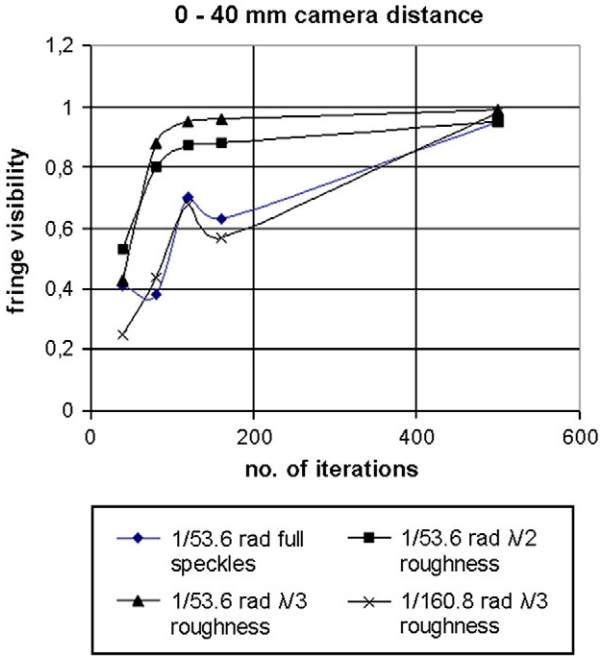

Fig. 5. Fringe visibility of the interference pattern of two phase retrieved waves in a near-field simulation versus the iteration. ("500 steps" points correspond to the visibility of the original complex waves, i.e., the target of phase retrieval, and the upper limit of the curves).

5. Experimental results

5.1. Far-field setup

Fig. 6 shows the (parallel) interferometric fringes of a rigid body rotation in a "far-field" experiment, where the object-to-camera distance was 70–72 cm. The object size was 40 mm×40 mm, and 2×20 recordings were used with a 1 mm step length. The visibility of the fringes is about 0.1 (after 400 iteration steps per wave), which is rather low. Besides, the amplitude characteristics of the object are well reconstructed by phase retrieval, i.e., shadows of the screws, and glazes on their head. Retrieving a good object amplitude contrast is an easier task than retrieving also the phase really correctly. According to Fig. 6 one must carefully define what is meant by "successful phase retrieval." One interpretation is that the obtained phase of the objective speckle field enables the beam to be focused somewhere into point sources. The other interpretation requires also the relative phase of these point sources to be correct. The conclusion is that the visibility of interferometric fringes is a very sensitive measure of convergence, as it includes information about the mentioned relative phases as well. The low visibility in Fig. 6 means that the far-field setup combined with iterative phase retrieval has low quality results, but this is not the only possible setup.

5.2. Imaging setup

Experiments done with the imaging setup in Fig. 2 are more promising. Fig. 7 shows the interferometric fringes of a displacement due to a central load, when the image-to-camera distance was −10–10 mm. The object size was 40 mm×40 mm as before, and 2×20 recordings were used with a 1 mm step length. The magnification of the imaging was set so that the

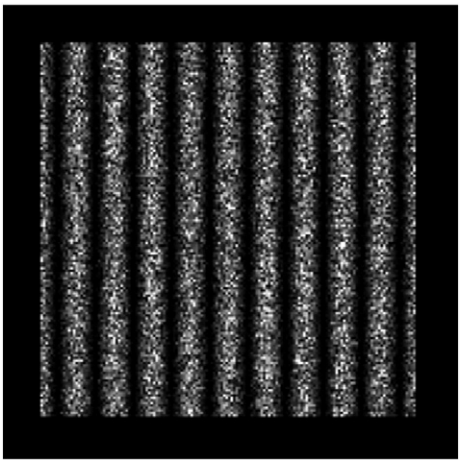

Fig. 4. Interference pattern of a rotated diffuse and small object in a near-field simulation. The fringe visibility is above 0.9.

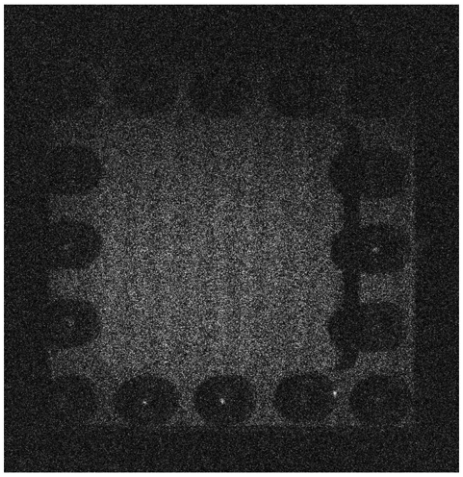

Fig. 6. Interference pattern of a rotated diffuse and large object in a far-field setup experiment. The fringe visibility is about 0.1.

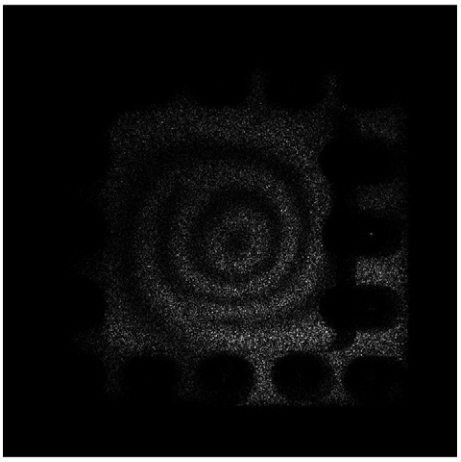

Fig. 7. Interference pattern of a centrally loaded diffuse and large object in an imaging setup experiment. The fringe visibility is above 0.5. Note that the fringe system is incorrect.

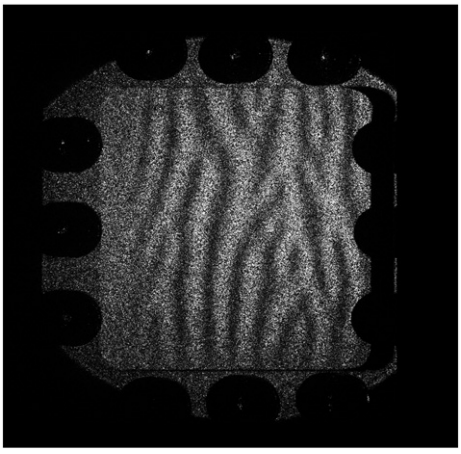

Fig. 8. Incorrect fringes of a rigid body rotation in the imaging setup.

image should fit well inside the CCD area (cca. 6.7 mm × 6.7 mm), and the F# of the lens (Pancolar 50 mm 1:1.8 photo objective) was set to 16 to have resolvable speckles. The visibility of the fringes is above 0.5 (after 400 iteration steps per wave), which is satisfactory for further fringe processing. However, the fringe system obtained is *incorrect*: the fringes of a real displacement field should *never* split or have an end, meaning ambiguous displacement values and leading to interpretation problems. This weird effect was further analyzed in another case with the following results.

Even the "parallel" fringes of a rigid body rotation turn out to be incorrect, as it is shown in Fig. 8. By changing a relaxation parameter in the modulus projection, the fringe system varies, but remains incorrect. If the camera motion range is set directly behind the image plane (in the case of Fig. 7 the image plane intersects this range right in the middle), or 2 cm behind the image plane (this means a 2–4 cm image-to-camera distance), the fringes are still incorrect and have good visibility. If the range is further shifted to 5, 10 or 15 cm behind the image plane (and the F# of the lens is reduced accordingly to have still resolved speckles), the fringes are correct, but have low visibility again. Explaining this phenomenon requires further detailed investigation both experimentally and by simulations. Our preliminary concept about this phase error is that the combination of the lens aperture in the setup and phase retrieval itself as a method is responsible. Simulations of low-pass filtered deformable objects in the near-field setup showed that phase retrieval converges slower if filtering is applied, but the obtained fringe systems during the iteration did not really resemble to Figs. 7 or 8. Note that the F# of the lens being as large as 16 (thus having a small aperture) alone is not enough to have incorrect fringes, otherwise ESPI or imaging digital holographic interferometry would not work. Fig. 6 also means that phase retrieval alone is also not enough to have incorrect fringes.

6. Summary

We have showed that it is possible to obtain interferometric fringes of the displacement field of loaded diffuse objects as large as 40 mm from two sets of intensity recordings by means of iterative phase retrieval, but either the visibility or the structure of the fringes in experiments is poor. Fringe visibility measures the convergence of phase retrieval more accurately, than simple intensity correlation or solo object intensity contrast. The most promising results were obtained using an imaging setup, but the origin of the resulting erroneous phase structure must be understood much better in the future. A preliminary concept about this error is that the lens aperture has an effect on phase retrieval methods in certain cases of imaging setup geometry.

References

[1] T. Zhang, I. Yamaguchi, Opt. Lett. 23 (1998) 1221.
[2] U. Schnars, W.P.O. Jüptner, Meas. Sci. Technol. 13 (2002) R85.
[3] S. Schedin, J. Holo. Speckle 3 (2006) 1.
[4] B. Gombkötő, J. Kornis, Z. Füzessy, Opt. Commun. 214 (2002) 115.
[5] B. Gombkötő, J. Kornis, Z. Füzessy, M. Kiss, P. Kovács, Appl. Opt. 43 (2004) 1621.
[6] J.R. Fienup, Appl. Opt. 21 (1982) 2758.
[7] P.F. Almoro, G. Pedrini, W. Osten, Appl. Opt. 45 (2006) 8596.
[8] P.F. Almoro, G. Pedrini, A. Anand, W. Osten, S.G. Hanson, Appl. Opt. 48 (2009) 932.
[9] J.R. Fienup, Opt. Lett. 3 (1978) 27.
[10] D.R. Luke, Inverse Prob. 21 (2005) 37.
[11] M.R. Teague, J. Opt. Soc. Am. 73 (1983) 1434.
[12] G. Pedrini, P. Froning, H.J. Tiziani, F.M. Santoyo, Opt. Commun. 164 (1999) 257.
[13] L.J. Allen, M.P. Oxley, Opt. Commun. 199 (2001) 65.
[14] P.F. Almoro, S.G. Hanson, Opt. Exp. 16 (2008) 7608.